

UC Berkeley

UC Berkeley Previously Published Works

Title

Identifying surface structural changes in a newly-developed Ga-based alloy with melting temperature below 10 °C

Permalink

<https://escholarship.org/uc/item/4n08d2h8>

Authors

Yu, Qing
Zhang, Qiubo
Zong, Junjie
et al.

Publication Date

2019-10-01

DOI

10.1016/j.apsusc.2019.06.203

Peer reviewed

Identifying surface structural changes in a newly-developed Ga-based alloy with melting temperature below 10 °C

Qing Yu^{1,2,*}, Qiubo Zhang^{3,*}, Junjie Zong^{1,2}, Suyu Liu^{1,2}, Xuelin Wang^{1,2}, Xiaodong Wang^{1,2}, Haimei Zheng^{3,4,§}, Qingping Cao^{1,2}, Dongxian Zhang⁵, Jian-Zhong Jiang^{1,2,§}

¹International Center for New-Structured Materials (ICNSM), Laboratory of New-Structured Materials, School of Materials Science and Engineering, Zhejiang University, Hangzhou, 310027, People's Republic of China.

²State Key Laboratory of Silicon Materials, Zhejiang University, Hangzhou, 310027, People's Republic of China.

³Materials Science Division, Lawrence Berkeley National Laboratory, Berkeley, California 94720, United States.

⁴Department of Materials Science and Engineering, University of California, Berkeley, Berkeley, California 94720, United States.

⁵State Key Laboratory of Modern Optical Instrumentation, Zhejiang University, Hangzhou, 310027, People's Republic of China

*These authors contributed equally to this work.

§ Corresponding author: jiangjz@zju.edu.cn and hmzheng@lbl.gov

Abstract

Surface oxidation, as one of fundamental chemical reactions in metals, greatly affects their properties. Herein, we develop a new quaternary GaInSnZn liquid metal with the melting temperature of 9.7 °C, which is the lowest among all reported Ga-based liquid metals. With high-resolution transmission electron microscopy, we directly observed the oxide layer formed on the surface of the liquid metal. The initially formed oxide layer is revealed to be amorphous and very sensitive to electron beam. Prolonged irradiation results in its structural change from amorphous to crystalline phases. The present finding refreshes the basic understanding of surface oxidization of liquid metals and opens up the possibility of tuning surface structures and morphologies by using electron beam irradiation.

Introduction

Ga-based liquid metals, especially gallium and its eutectic alloys (EGaIn and EGaInSn), have been becoming a hot research topic in biomimetic^[1], chemical^[2], biomedical^[3], electrical^[4] and material science^[5] owing to their fluidity with low viscosity at temperatures above 20 °C together with superior thermal and electrical conductivities. More importantly, they feature non-toxicity, very low evaporation pressure and the ability to form a functional oxide layer on the surface^[6,7], which enable them intriguing for practical applications in flexible and stretchable electronics^[4,8,9], direct writing^[8], 3D printing^[10], catalysts^[11-13], actuators^[14], microfluidics^[15,16], reconfigurable devices^[17,18] and chip cooling^[19,20]. Development of new Ga-based alloys with even lower melting temperature is always desirable, which will further extend temperature range for their applications. When the Ga-based liquid metal is exposed to ambient atmosphere, a thin self-limiting oxide layer can spontaneously and rapidly form on the surface. Consequently, it significantly changes the bulk behavior of liquid metal along with its surface tension and wetting^[21-23], allowing the liquid metal to adhere to almost any solid surface and providing a new insight to manipulate the liquid-metal structure for specific applications^[22,24-27]. For example, Khan et al. recently reported an approach to tune the interfacial tension of an EGaIn via electrochemical deposition (or removal) of an oxide layer on its surface using external electrical field^[22]. Hu et al. also successfully realized the morphological manipulations of an EGaInSn (Galinstan) in an alkaline electrolyte on a graphite surface via electrochemical reaction^[25]. Their underlying mechanism is due to the quick formation of oxide layer on the liquid metal that greatly changes surface tension and causes dramatic transformation between various morphologies. Apart from surface shaping, very recently, the oxide layer on the surface of liquid metals has also attracted increasing attentions due to the enormous potential for the synthesis of low-dimensional compounds of oxides^[12,13,28]. Taking advantage of the formation of a thin

surface oxide of liquid gallium, Syed et al. fabricated gallium oxide nanoflakes by direct sonication of liquid gallium in deionized water and subsequent annealing^[13]. Zavabeti et al. synthesized atomically thin metal oxides (HfO_2 , Al_2O_3 and Gd_2O_3)^[28] and ultrathin nanosheets and nanofibers of boehmite^[12] by utilizing Ga-based liquid metals as an excellent reaction media. Although the significance of surface oxidation of liquid metals has been recognized for long, however, the basic question, i.e., what is the structure of oxide layer on the surface of Ga-based liquid metals, still remains unsolved, which is essential for the exploration and development of the future practical applications of Ga-based liquid metals.

Earlier experiments on the oxidation of liquid pure Ga suggested that a thin self-limiting oxide layer almost instantly forms even in the environments with mere few ppm levels of oxygen^[29]. Through controlling oxygen dosage under UHV conditions, Regan et al proposed that the gallium oxide layer on the surface of liquid Ga is 0.5 nm-thick solid with amorphous or poorly crystallized structure revealed by using X-ray scattering technique on a curved surface^[30]. The authors strongly suggested to re-examine the surface layer structure on a sample with flat surface^[30]. When exposed in air, Plech et al. found the thickness of oxide layer increases up to 3 nm^[31]. The presence of thin surface oxide layer can protect bulk liquid from further oxidation, like aluminum^[32]. However, in the current literatures, the characterization of Ga-based liquid metal surface oxides mainly focused on their compositions by XPS technique^[16,23,33], while direct experimental evidences, e.g., transmission electron microscopy (TEM), for their structures are still missing.

Here we develop a new Ga-based liquid metal, containing In, Sn and Zn additional elements (hereafter named GISZ), which exhibits the lowest melting temperature than previously reported for Ga-based liquid metals. The structural evolution of their surface oxide layers of the GISZ liquid has been investigated by using high-resolution TEM. An amorphous oxide layer formed on the surface of GISZ liquid is directly observed. We reveal that the structure of the surface oxide layer can be adjusted by electron beam, i.e.,

prolonged irradiation leads to crystallization of the amorphous surface oxide layer. The development of new Ga-based multi-component liquid metals is useful to extend their applications, while determination of the surface oxide layer of Ga-based multi-component liquid metals would be beneficial to understand the surface oxidation and provide guidance for surface manipulation by using external fields.

Experimental

Preparation of sample: For preparation of GISZ alloys, pure gallium, indium, tin and zinc with purity higher than 99.99 at. % were used. The mixtures of GISZ alloys with various compositions were sealed in quartz tubes under a vacuum of $\sim 5 \times 10^{-4}$ Pa and heated at 250 °C for a few hours until complete melting in a thermostatic oil bath. After melting, the alloys were cooled to room temperature and transferred into sealed vials using a plastic transfer pipette for further use.

DSC and XPS measurements: The thermal behaviors of GISZ liquid metals were investigated by using a PerkinElmer Diamond DSC at a heating and cooling rate of 10 K/min over the temperature range of -40 to 50 °C. X-ray photoelectron spectroscopy (XPS) measurements were carried out to determine the composition of surface oxide using an AXIS Supra spectrometer under ultra-high vacuum (UHV) conditions (10^{-9} mTorr). A monochromated Al K_{α} X-ray source (1486.6 eV energy) was used with a spot size of about $300 \times 700 \mu\text{m}^2$ operated at an emission current 8 mA and an anode voltage of 15 kV. The scanning was performed over a $160 \times 160 \mu\text{m}^2$ area with a pass energy of 40 eV. The sample was touched using a double-sided tape that are coated onto copper substrate, and then transferred into the UHV chamber. All spectra were calibrated using C 1s peak (binding energy of 284.8 eV) and subsequent analyses were performed by using ESCApe software.

TEM Characterization and EDS mapping: The TEM samples were prepared by sucking a small amount of GISZ liquid metal using a pipette, and

slightly extruding at the tip to quickly slide on the carbon-coated copper grids. Basic microstructural characterizations of surface oxide were performed using a Cs-corrected TEM (FEI ThemIS 60-300) operating with an acceleration voltage of 300 kV in the National Center for Electron Microscopy of Lawrence Berkeley National Laboratory. The composition of oxide was determined by energy-dispersive x-ray spectroscopy (EDS) using ThemIS equipped with Bruker Super-X EDS detector. To study the structural evolution of surface oxide layer, high energy parallel electron beam was used.

Results and Discussion

When gallium is alloyed with indium and tin to form eutectic alloys of EGaIn and EGaInSn (Galinstan), the melting temperature is reduced gradually^[34,35]. Zinc has a high solubility in gallium, forming a eutectic alloy of EGaZn by the addition of 3.9 at. % Zn^[36]. It is reasonable to assume that the melting temperature of liquid metal can be further reduced when the fourth element is added. Therefore, we synthesized a series of quaternary alloys of GISZs with various concentrations. As a result, the GISZ alloy with even lower melting temperature is successfully developed, as confirmed by DSC results in Fig. 1. For comparison, the DSC data for pure Ga, EGaIn as well as Galinstan are also presented. Obviously, with the sequential addition of In, Sn and Zn, all the onset temperature, $T_{m-onset}$, peak temperature, T_{m-p} , and end temperature, T_{m-end} , of melting of Ga-based metals characterized by a broad endothermic peak during heating shift toward to lower temperatures. The melting temperature data obtained here for Ga, EGaIn and Galinstan are very close to the corresponding data available in the literature^[37-42] as summarized in Table. 1, while GISZ has the lowest melting peak temperature of 9.7 °C than those previously reported for Ga-based liquid metals. In addition, the cooling process reveals that the freezing temperature as indicated by the sharp crystallization peak also gradually reduced while alloying with In and Sn. Although further adding Zn element seems not cause a continuous decrease in freezing temperature, the freezing temperature

achieved is actually very low, approaching to $-20\text{ }^{\circ}\text{C}$. Furthermore, our synthesized quaternary alloy possesses higher electrical and thermal conductivities compared with eutectic GaIn and Galinstan alloys, as listed in Table 1, which evidently indicates that the Zn addition allows the liquid metal to retain in liquid state at very low temperatures, thus extending its use in low-temperature fields, especially for electronic and refrigeration applications.

To study the room temperature surface oxides of GISZ, we have employed high-resolution TEM characterization combined with EDS analyses. The TEM imaging shows that GISZ retains in liquid state and a variety of morphologies including particles, platelet and rods are observed. Figure 2(a) gives the TEM image of one individual liquid metal particle that can exist stably by hanging on carbon support. Obvious core-shell morphology is observed. The outer shell is considered to be the surface oxide layer^[33] with the thickness of about 3.7 nm. The corresponding fast Fourier transformation (FFT) pattern of the particle in Fig. 2(b) displays an amorphous diffraction ring, indicating that the thin oxide layer encapsulating the free surface of liquid GISZ is amorphous, similar with previous reports in gallium and Galinstan^[28,30] that found a self-limiting amorphous gallium oxide was formed on the surface. High-angle annular dark field (HAADF) STEM image as shown in Fig. 3(a) reveals non-uniform contrast, and the outer oxide layer has lower intensity than the core. Energy dispersive X-ray spectroscopy (EDS) elemental mapping in Figs. 3(b-f) reflect the distribution of Ga (red), In (blue), Sn (green), Zn (yellow) and O (cyan), respectively, which indicate Ga, In, Sn, Zn element is uniformly distributed in the core of particle, but the surface oxide layer is mainly composed of Ga, Zn and O. The same results are observed for the rod-like sample in Fig. S1.

To further determine the chemical composition of surface oxide layer of GISZ, we performed XPS measurements for both Galinstan and GISZ alloys. As shown in Fig. 4, in addition to strong Ga peaks (2p, 3p and 3d) and O peak (1s), adventitious C peak (1s), weak In peaks (3d) as well as Sn peaks (3d) in

the survey XPS spectra of two alloys, obvious Zn peaks (2p) are observed in GISZ, confirming the presence of Ga, Zn and O in the surface oxide of GISZ. High resolution fits of Ga 2p, In 3d, Sn 3d, Zn 2p and O 1s spectra of GISZ are given in Fig. S2 to investigate their chemical bonding states. The Ga 2p spectra are split into two peaks. The less intense peaks located at binding energy of 1115.8 eV and 1142.7 eV, respectively, correspond to the Ga 2p peaks of metallic gallium (Ga^0)^[43] from deeper penetration of metallic liquid. The more intense peaks centered at 1117.7 eV and 1144.6 eV, respectively, can be attributed to the valence state Ga 2p (Ga^{3+}) in oxide^[43]. The In 3d and Sn 3d spectra indicate that the two elements are primarily in metallic states, excited from the metallic liquid beneath the surface layer. For Zn, the peaks located at 1021.8 eV and 1044.8 eV correspond to Zn $2p_{3/2}$ and Zn $2p_{1/2}$ states, respectively. Since Zn $2p_{3/2}$ peak showed a small shift of about 0.4 eV between the metallic (Zn^0) and oxidation (Zn^{2+}) states, it is really hard to distinguish them from present Zn 2p spectra^[44,45]. But according to the thermodynamic points, ZnGa_2O_4 has the standard molar enthalpy of formation at 298 K of $-1473 \text{ kJ}\cdot\text{mol}^{-1}$ ^[46], which is considerably more stable than gallium oxide ($-1089.1 \text{ kJ}\cdot\text{mol}^{-1}$) and zinc oxide ($-350.5 \text{ kJ}\cdot\text{mol}^{-1}$)^[47], suggesting that ZnGa_2O_4 might be preferentially formed on the surface of liquid GISZ alloy. In addition, Phani et al. ^[48]found the energetic separation (ΔE) between the Zn $2p_{3/2}$ and Ga $2p_{3/2}$ peaks can be used as a sensitive tool to distinguish between a complete formation of ZnGa_2O_4 compounds (lower ΔE than 96.3 eV) and a mixture of zinc oxide and gallium oxide powers. Here the ΔE is determined to be 95.9 eV, thus it can be speculated that the surface oxide is more likely to contain ZnGa_2O_4 only^[49,50]. As for O 1s spectrum in Fig. S2, it displays double peaks, where the low binding energy peak situated at about 530.5 eV can be ascribed to Ga-O and Zn-O bonds, the high binding energy peak around 532 eV is usually attributed to chemisorbed or dissociated oxygen or OH species on the surface^[44,45].

Furthermore, TEM, as one powerful characterization method, not only provides a platform for spatially imaging at the atomic scale, chemical

6

analysis and diffraction, but also makes it possible to create defects and induce phase transitions of materials by electron beam irradiation^[51-53]. Therefore, to explore the effect of electron beam on the structure of surface oxide layer, prolonged parallel electron beam irradiation was performed at a chosen region with a flux of $1.09 \times 10^6 \text{ e nm}^{-2} \text{ s}^{-1}$. A series of high-resolution TEM images with irradiation time and corresponding FFT patterns were presented in Fig. 5. Figure 5(a) is the first image (0 min) taken right after the area was exposed to electron beam, evidently revealing that the initial surface oxide layer is entirely amorphous. After 4 minutes of exposure to electron beam in Fig. 5(b), some visible fringes begin to occur on the original rough surface, but the FFT pattern still shows amorphous ring, suggesting that surface atoms of oxide layer develop well-defined lamellar structures but without obvious in-plane positional order. Further increasing irradiation time, surface crystalline structure can be clearly observed, and several diffraction spots are superimposed on the FFT patterns as shown in Figs. 5(c) and 5(d) (highlighted with circles). In addition, the thickness of oxide layer increases slightly under irradiation. In order to reexamine the effect of electron beam on the surface morphology of GISZ, the same illumination process was repeated in another region of sample as shown in Fig. S3. Similarly, the area of the initial illumination is completely amorphous, and the sample is relatively uniform. After 3 minutes of exposure, the prominent particle-like contrasts start to appear. As the irradiation proceeds, the image contrasts become much stronger and some ordered structures are detected within the particles after 20 minutes of exposure. Figure. 6 gives the higher magnification TEM images of three representative ordered regions and corresponding FFT patterns, showing very clear lattice fringes with interplanar d -spacing distances of about 0.15 nm, 0.21 nm and 0.26 nm, that may correspond to the (044), (004) and (113) facets of cubic ZnGa_2O_4 , respectively. It is revealed that the surface oxide layer is very sensitive to the electron beam, and prolonged irradiation leads to structural change of ZnGa_2O_4 from amorphous to crystalline phases. ZnGa_2O_4 , as a wide band gap

semiconductor, has also attracted enormous attention due to its wide application prospect in photocatalyst, electroluminescence and field emission displays^[49,54]. However, the commonly used method to synthesize ZnGa₂O₄ is the solid-state reaction between ZnO and Ga₂O₃, which requires long-term heat treatment at a considerably high temperature^[48,54]. Therefore, our finding provides a possibility for synthesizing low-dimensional ZnGa₂O₄ at room temperature by electron beam irradiation.

Conclusions

In this study, a new quaternary liquid metal (GaInSnZn) with a melting temperature of 9.7 °C, which was the lowest one among all reported Ga-based metals, was developed, and its structure of surface oxide layer was investigated. The high resolution TEM imaging gives a direct observation of the core-shell structure constructed by liquid metal-oxide layer, and clearly confirms that the initially formed surface oxide is amorphous. Combined with EDS and XPS measurements, we find that the oxide layer is primarily composed of Ga, Zn and O. In addition, the amorphous oxide layer can be tuned by electron beam irradiation, which can give rise to the structural transition of oxide layer from amorphous to crystalline phases. Since electron beam irradiation time and scanning area can be controlled easily, it would be extremely intriguing to intentionally manipulate the surface morphology or even synthesize low-dimensional semiconductors on the surface of liquid metals by electron irradiation.

Acknowledgements

Financial supports from the National Natural Science Foundation of China (U1832203, U1532115, 51671170 and 51671169), the National Key Research and Development Program of China (2016YFB0701203, 2016YFB0700201, and 2017YFA0403400), the NSF of Zhejiang Province (Z1110196, Y4110192 and LY15E010003), and the Fundamental Research Funds for the Central Universities are gratefully acknowledged. H.Z. thanks the support from U.S. Department of Energy, Office of Science, Office of

Basic Energy Sciences, Materials Sciences and Engineering Division under Contract No. DE-AC02-05-CH11231 within the KC22ZH program.

References:

- [1] J. Zhang, Y. Yao, L. Sheng, and J. Liu, *Self-Fueled Biomimetic Liquid Metal Mollusk*, *Adv. Mater.* **27**, 2648-2655 (2015).
- [2] T. Daeneke, K. Khoshmanesh, N. Mahmood, I. A. de Castro, D. Esrafilzadeh, S. J. Barrow, M. D. Dickey, and K. Kalantar-Zadeh, *Liquid metals: fundamentals and applications in chemistry*, *Chem. Soc. Rev.* **47**, 4073-4111 (2018).
- [3] J. Yan, Y. Lu, G. Chen, M. Yang, and Z. Gu, *Advances in liquid metals for biomedical applications*, *Chem. Soc. Rev.* **47**, 2518-2533 (2018).
- [4] Y. Gao *et al.*, *Wearable Microfluidic Diaphragm Pressure Sensor for Health and Tactile Touch Monitoring*, *Adv. Mater.* **29**, 1701985 (2017).
- [5] A. d. C. I *et al.*, *A Gallium-Based Magnetocaloric Liquid Metal Ferrofluid*, *Nano Lett.* **17**, 7831-7838 (2017).
- [6] M. D. Dickey, *Emerging applications of liquid metals featuring surface oxides*, *ACS Appl. Mater. Interfaces* **6**, 18369-18379 (2014).
- [7] S.-Y. Tang *et al.*, *Functional Liquid Metal Nanoparticles Produced by Liquid-Based Nebulization*, *Adv. Mater. Technol.* **4**, 1800420 (2019).
- [8] J. W. Boley, E. L. White, G. T. C. Chiu, and R. K. Kramer, *Direct Writing of Gallium-Indium Alloy for Stretchable Electronics*, *Adv. Funct. Mater.* **24**, 3501-3507 (2014).
- [9] M. D. Dickey, *Stretchable and Soft Electronics using Liquid Metals*, *Adv. Mater.* **29** (2017).
- [10] C. Ladd, J. H. So, J. Muth, and M. D. Dickey, *3D printing of free standing liquid metal microstructures*, *Adv. Mater.* **25**, 5081-5085 (2013).
- [11] S.-T. Liang, H.-Z. Wang, and J. Liu, *Progress, Mechanisms and Applications of Liquid-Metal Catalyst Systems*, *Chem. Eur. J.* **24**, 17616-17626 (2018).
- [12] A. Zavabeti *et al.*, *Green Synthesis of Low-Dimensional Aluminum Oxide Hydroxide and Oxide Using Liquid Metal Reaction Media: Ultrahigh Flux Membranes*, *Adv. Funct. Mater.* **28**, 1804057 (2018).

- [13] N. Syed *et al.*, *Sonication-Assisted Synthesis of Gallium Oxide Suspensions Featuring Trap State Absorption: Test of Photochemistry*, *Adv. Funct. Mater.* **27**, 1702295 (2017).
- [14] L. Russell, J. Wissman, and C. Majidi, *Liquid metal actuator driven by electrochemical manipulation of surface tension*, *Appl. Phys. Lett.* **111**, 254101 (2017).
- [15] K. Khoshmanesh, S.-Y. Tang, J. Y. Zhu, S. Schaefer, A. Mitchell, K. Kalantar-zadeh, and M. D. Dickey, *Liquid metal enabled microfluidics*, *Lab Chip* **17**, 974-993 (2017).
- [16] M. D. Dickey, R. C. Chiechi, R. J. Larsen, E. A. Weiss, D. A. Weitz, and G. M. Whitesides, *Eutectic Gallium-Indium (EGaIn): A Liquid Metal Alloy for the Formation of Stable Structures in Microchannels at Room Temperature*, *Adv. Funct. Mater.* **18**, 1097-1104 (2008).
- [17] J. Wang, S. Liu, and A. Nahata, *Reconfigurable plasmonic devices using liquid metals*, *Opt. Express* **20**, 12119-12126 (2012).
- [18] J. Wang, S. Liu, S. Guruswamy, and A. Nahata, *Reconfigurable liquid metal based terahertz metamaterials via selective erasure and refilling to the unit cell level*, *Appl. Phys. Lett.* **103** (2013).
- [19] K. Ma and J. Liu, *Liquid metal cooling in thermal management of computer chips*, *Front. Energy Power Eng. China* **1**, 384-402 (2007).
- [20] J. Y. Zhu, S. Y. Tang, K. Khoshmanesh, and K. Ghorbani, *An Integrated Liquid Cooling System Based on Galinstan Liquid Metal Droplets*, *ACS Appl. Mater. Interfaces* **8**, 2173-2180 (2016).
- [21] R. J. Larsen, M. D. Dickey, G. M. Whitesides, and D. A. Weitz, *Viscoelastic properties of oxide-coated liquid metals*, *J. Rheol.* **53**, 1305-1326 (2009).
- [22] M. R. Khan, C. B. Eaker, E. F. Bowden, and M. D. Dickey, *Giant and switchable surface activity of liquid metal via surface oxidation*, *Proc. Natl. Acad. Sci. USA* **111**, 14047-14051 (2014).

- [23] F. Scharmann, G. Cherkashinin, V. Breternitz, C. Knedlik, G. Hartung, T. Weber, and J. A. Schaefer, *Viscosity effect on GaInSn studied by XPS*, Surf. Interface Anal. **36**, 981-985 (2004).
- [24] Z. Yu, Y. Chen, F. F. Yun, D. Cortie, L. Jiang, and X. Wang, *Discovery of a Voltage-Stimulated Heartbeat Effect in Droplets of Liquid Gallium*, Phys. Rev. Lett. **121**, 024302 (2018).
- [25] L. Hu, L. Wang, Y. Ding, S. Zhan, and J. Liu, *Manipulation of Liquid Metals on a Graphite Surface*, Adv. Mater. **28**, 9210-9217 (2016).
- [26] S. Runde, H. Ahrens, F. Lawrenz, A. Sebastian, S. Block, and C. A. Helm, *Stable 2D Conductive Ga/Ga(OxHy) Multilayers with Controlled Nanoscale Thickness Prepared from Gallium Droplets with Oxide Skin*, Adv. Mater. Interfaces **5**, 1800323 (2018).
- [27] T. Hutter, W.-A. C. Bauer, S. R. Elliott, and W. T. S. Huck, *Formation of Spherical and Non-Spherical Eutectic Gallium-Indium Liquid-Metal Microdroplets in Microfluidic Channels at Room Temperature*, Adv. Funct. Mater. **22**, 2624-2631 (2012).
- [28] A. Zavabeti et al., *A liquid metal reaction environment for the room-temperature synthesis of atomically thin metal oxides*, Science **358**, 332-335 (2017).
- [29] T. Liu, P. Sen, and C.-J. Kim, *Characterization of Nontoxic Liquid-Metal Alloy Galinstan for Applications in Microdevices*, J. Microelectromech. Syst. **21**, 443-450 (2012).
- [30] M. J. Regan, H. Tostmann, P. S. Pershan, O. M. Magnussen, E. DiMasi, B. M. Ocko, and M. Deutsch, *X-ray study of the oxidation of liquid-gallium surfaces*, Phys. Rev. B **55**, 10786-10790 (1997).
- [31] A. Plech, U. Klemradt, H. Metzger, and J. Peisl, *In situ x-ray reflectivity study of the oxidation kinetics of liquid gallium and the liquid alloy*, J. Phys.: Condens. Matter **10**, 971-982 (1998).
- [32] N. N. Greenwood and A. Earnshaw, *Chemistry of the Elements* (Pergamon, New York, 1984).

- [33] D. Kim, P. Thissen, G. Viner, D.-W. Lee, W. Choi, Y. J. Chabal, and J.-B. Lee, *Recovery of Nonwetting Characteristics by Surface Modification of Gallium-Based Liquid Metal Droplets Using Hydrochloric Acid Vapor*, ACS Appl. Mater. Interfaces **5**, 179-185 (2012).
- [34] A. T.J and A. I, *The Ga-In (Gallium-Indium) System*, J. Phase Equilib. **12**, 64-72 (1991).
- [35] A. Qusba, A. K. RamRakhyani, J.-H. So, G. J. Hayes, M. D. Dickey, and G. Lazzi, *On the Design of Microfluidic Implant Coil for Flexible Telemetry System*, IEEE Sens. J. **14**, 1074-1080 (2014).
- [36] , Ga-Zn Binary Phase Diagram 0-5 at.% Zn: Datasheet from "PAULING FILE Multinaries Edition-2012" in SpringerMaterials (https://materials.springer.com/isp/phase-diagram/docs/c_0104138), .
- [37] A. d. C. I et al., *A Gallium-Based Magnetocaloric Liquid Metal Ferrofluid*, Nano Lett **17**, 7831-7838 (2017).
- [38] T. Iida and R. I. L. Guthrie, *The Physical Properties of Liquid Metals* (Clarendon Press, Oxford, 1988).
- [39] K. C. Mills and Y. C. Su, *Review of surface tension data for metallic elements and alloys: Part 1 – Pure metals*, Inter. Mater. Rev. **51**, 329-351 (2013).
- [40] Y. Plevachuk, V. Sklyarchuk, S. Eckert, G. Gerbeth, and R. Novakovic, *Thermophysical Properties of the Liquid Ga-In-Sn Eutectic Alloy*, J. Chem. Eng. Data **59**, 757-763 (2014).
- [41] F. Carle, K. Bai, J. Casara, K. Vanderlick, and E. Brown, *Development of magnetic liquid metal suspensions for magnetohydrodynamics*, Phys. Rev. Fluids **2**, 013301 (2017).
- [42] D. Zrnica and D. S. Swatik, *On the resistivity and surface tension of the eutectic alloy of gallium and indium*, J. Less-Common Metals **18**, 67-68 (1969).
- [43] , NIST X-ray Photoelectron Spectroscopy Database, National Institute of Standards and Technology, 2000.

- [44] J. F. Moulder, W. F. Stickel, P. E. Sobol, and K. D. Bomben, *Handbook of X-Ray Photoelectron Spectroscopy: A Reference Book of Standard Spectra for Identification and Interpretation of XPS Data* (Physical Electronics, Eden Prairie, 1995).
- [45] G. E. Hammer and R. M. Shemanski, *The oxidation of zinc in air studied by XPS and AES*, *J. Vac. Sci. Technol. A* **1**, 1026-1028 (1983).
- [46] N. A. Gribchenkova, A. V. Steblevsky, and A. S. Alikhanyan, *Vaporization in the Ga₂O₃–ZnO system by high temperature mass spectrometry*, *J. Chem. Thermodynamics* **115**, 1-6 (2017).
- [47] L. D. R., *CRC Handbook of Chemistry and Physics* (CRC Press, 2018), 99 edn.
- [48] A. R. Phani, S. Santucci, S. Di Nardo, L. Lozzi, M. Passacantando, P. Picozzi, and C. Cantalini, *Preparation and characterization of bulk ZnGa₂O₄*, *J. Mater. Sci.* **33**, 3969-3973 (1998).
- [49] L. Zou, X. Xiang, M. Wei, F. Li, and D. G. Evans, *Single-Crystalline ZnGa₂O₄ Spinel Phosphor via a Single-Source Inorganic Precursor Route*, *Inorg. Chem.* **47**, 1361-1369 (2008).
- [50] B. K. Kang, H. D. Lim, S. R. Mang, K. M. Song, M. K. Jung, and D. H. Yoon, *Synthesis and characteristics of ZnGa₂O₄ hollow nanostructures via carbon@Ga(OH)CO₃@Zn(OH)₂ by a hydrothermal method*, *CrystEngComm* **17**, 2267-2272 (2015).
- [51] B. Wei *et al.*, *In Situ TEM Investigation of Electron Irradiation Induced Metastable States in Lithium-Ion Battery Cathodes: Li₂FeSiO₄ versus LiFePO₄*, *ACS Appl. Energy Mater.* **1**, 3180-3189 (2018).
- [52] A. V. Krashennnikov and K. Nordlund, *Ion and electron irradiation-induced effects in nanostructured materials*, *J. Appl. Phys.* **107**, 071301 (2010).
- [53] Z. Liu, Z. Fei, C. Xu, Y. Jiang, X.-L. Ma, H.-M. Cheng, and W. Ren, *Phase transition and in situ construction of lateral heterostructure of 2D superconducting α/β Mo₂C with sharp interface by electron beam irradiation*, *Nanoscale* **9**, 7501-7507 (2017).

[54] K. Ikarashi, J. Sato, H. Kobayashi, N. Saito, H. Nishiyama, and Y. Inoue, *Photocatalysis for Water Decomposition by RuO₂-Dispersed ZnGa₂O₄ with d10 Configuration*, J. Phys. Chem. B **106**, 9048-9053 (2002).

Table.1 Physical properties of several Ga-based liquid metals ^[37-42].

Liquid metals	Ga	EGaIn	Galinstan	GISZ
Density (g · cm ⁻³)	6.10	6.25	6.44	6.20
Melting Point at peak (°C)	29.8	15.7	13.2	9.7
Viscosity (10 ⁻³ Pa · S)	1.37	1.99	2.4	4.0
Surface tension (10 ⁻³ N · m ⁻¹)	718	624	585	639
Thermal conductivity (W · m ⁻¹ · K ⁻¹)	29.3	26.6	24.7	27.5
Electrical conductivity (10 ⁶ S · m ⁻¹)	3.7	3.4	3.5	3.9

Figure. 1

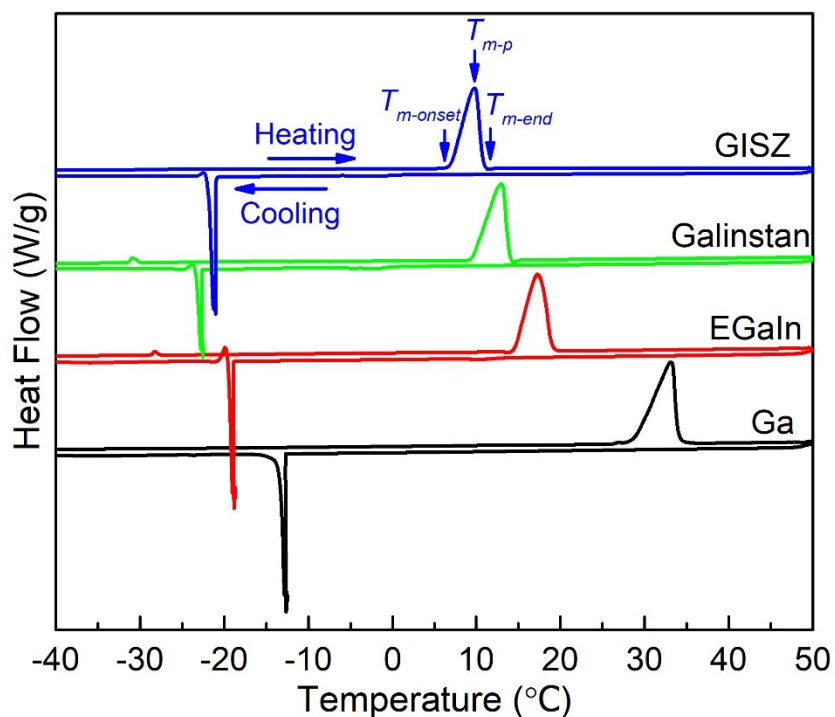


Figure. 1 DSC curves for pure Ga, eutectic Galn, Galinstan and GISZ alloys within the temperature range from -40 to 50 °C during heating and cooling at a rate of 10 K/min. $T_{m-onset}$, T_{m-p} and T_{m-p} represent the onset temperature, peak temperature and end temperature of melting.

Figure. 2

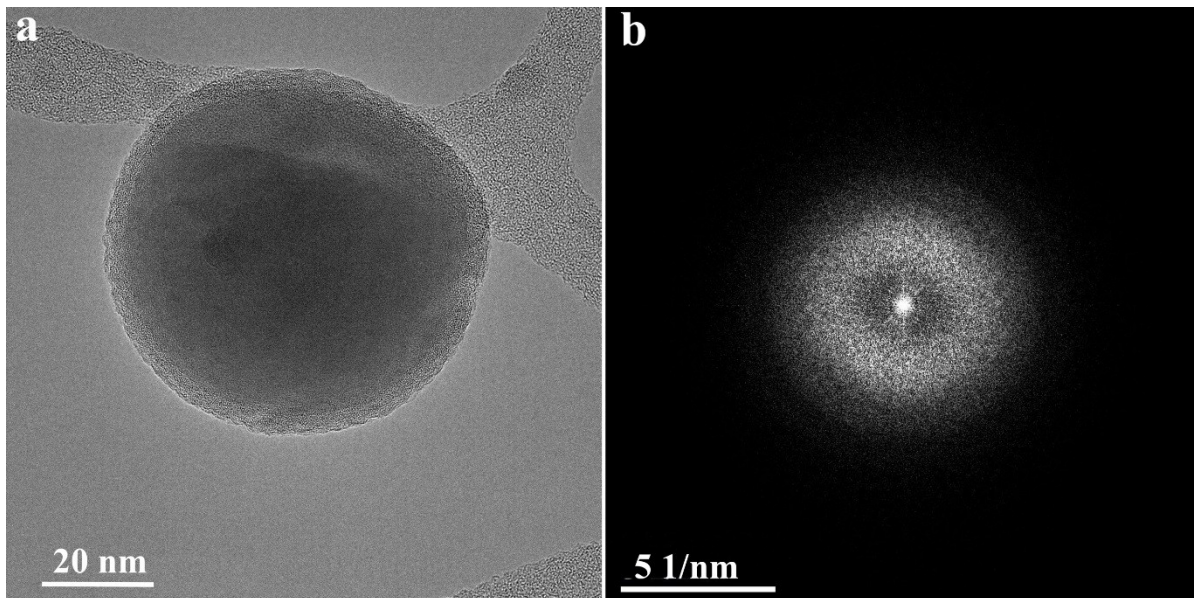


Figure. 2 (a) TEM image of one individual liquid metal particle and (b) corresponding FFT pattern.

Figure. 3

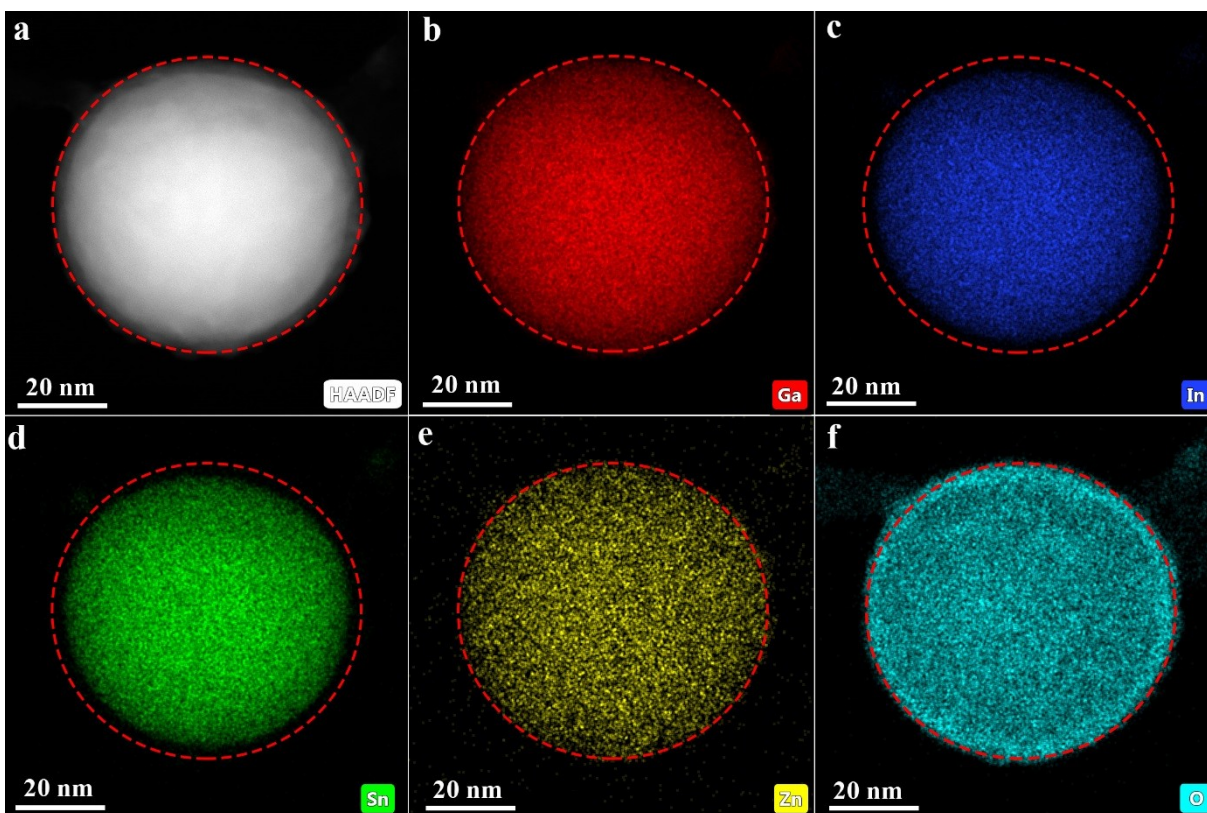


Figure. 3 Compositional characterization of one GISZ particle. (a) HAADF image and EDS mapping of (b) Ga in red, (c) In in blue, (d) Sn in green, (e) Zn in yellow and (f) O in cyan. The red dotted circles are to guide the eyes, indicating the difference in element distribution.

Figure. 4

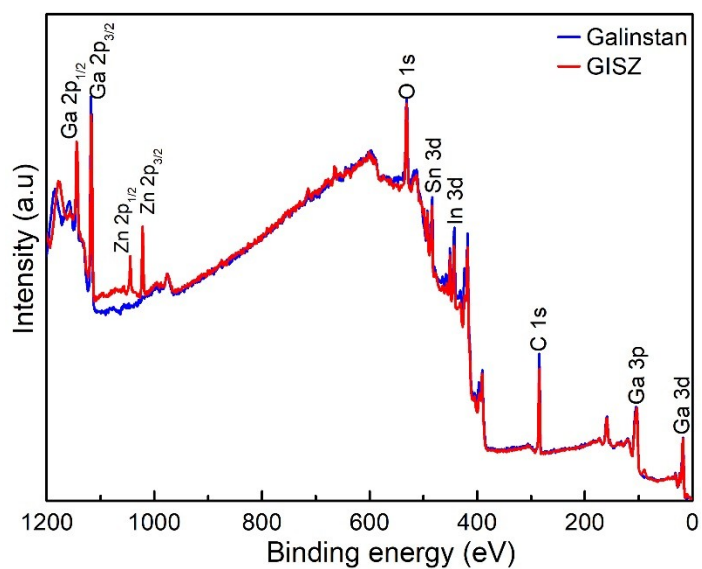


Figure. 4 Full-range survey XPS spectrum for the GISZ sample obtained in an AXIS Supra spectrometer using Al K_{α} X-ray. For comparison, XPS result of Galinstan was given.

Figure. 5

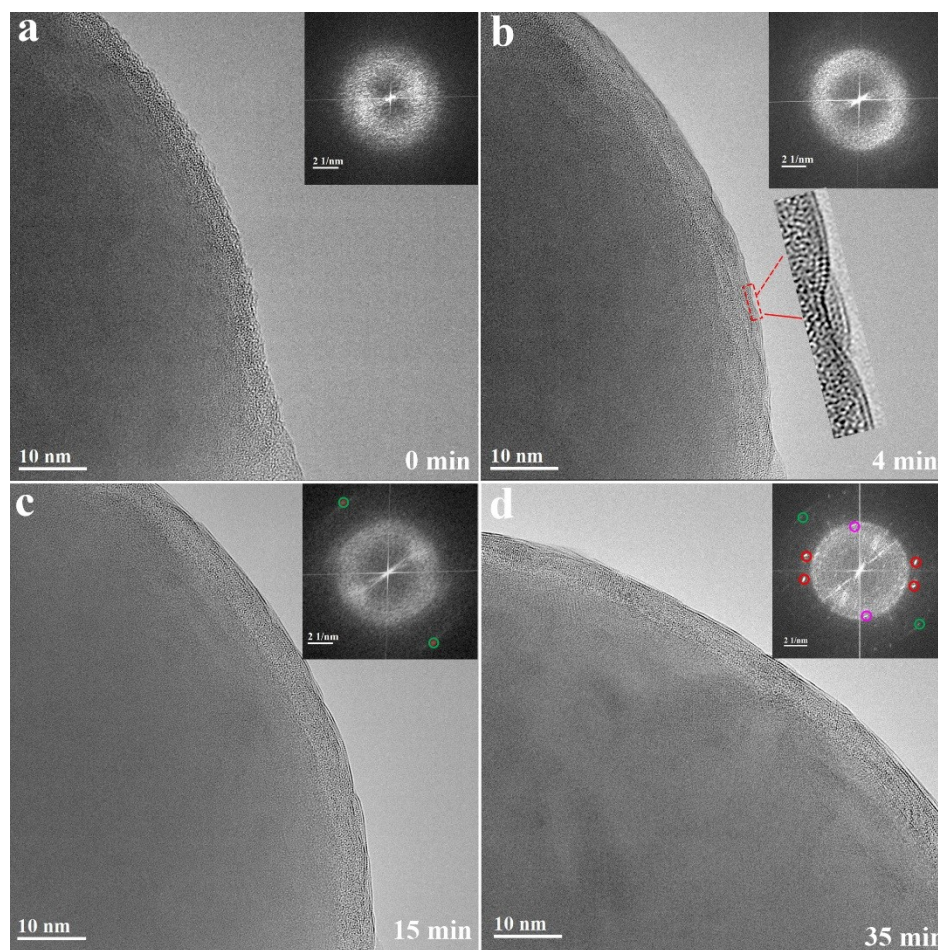


Figure. 5 Evolution of surface morphology of the GISZ sample with the increase of electron beam irradiation time. (a) TEM images (0 minute) acquired right after the area was exposed to electron beam. (b-d) TEM images corresponding to 4, 15 and 35 minutes of exposure, respectively.

Figure. 6

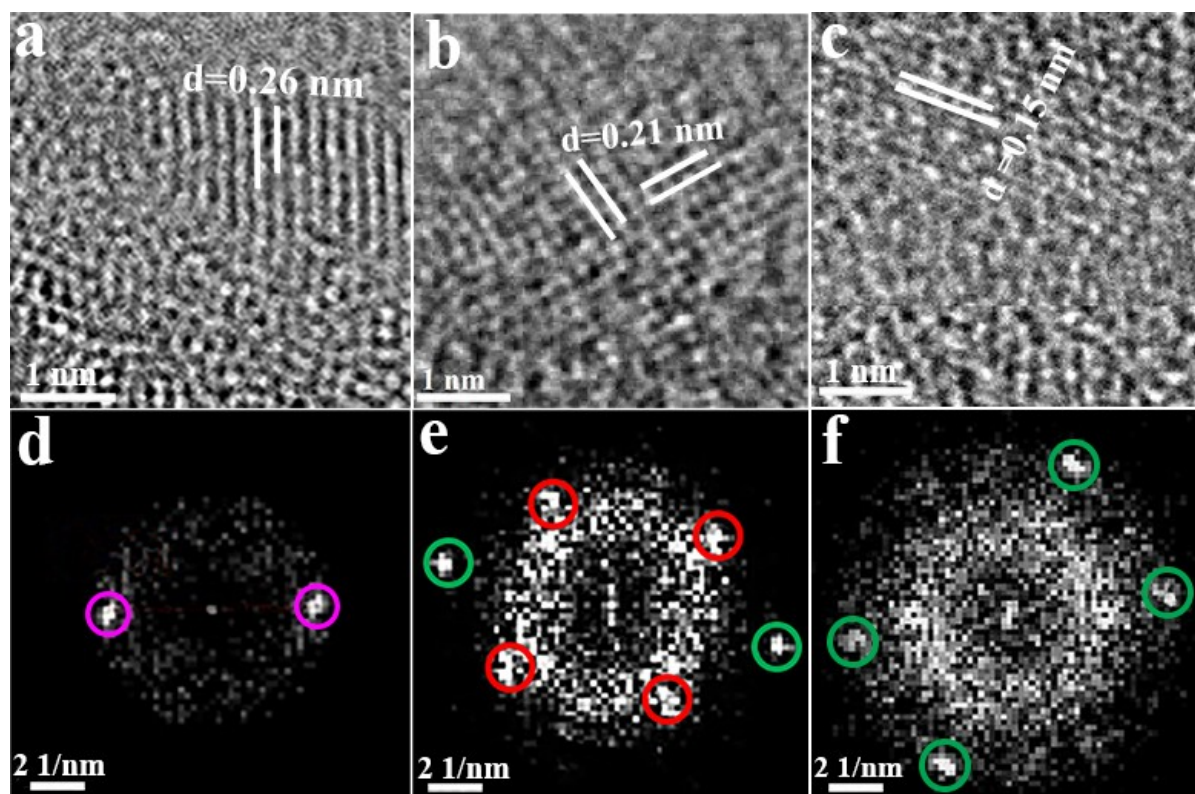


Figure. 6 (a-c) HRTEM images and (d-f) corresponding FFT patterns for three representative well-defined ordered regions, showing significant lattice fringes in surface layer of the GISZ sample after prolonged electron beam irradiation.